Journal of The Electrochemical Society, **150** (7) A933-A941 (2003)
0013-4651/2003/150(7)/A933/9/$7.00 © The Electrochemical Society, Inc.

Lithium Hectorite Clay as the Ionic Conductor in $LiCoO_2$ Cathodes

Michael W. Riley,* Peter S. Fedkiw,,z and Saad A. Khan**

Department of Chemical Engineering, North Carolina State University, Raleigh, North Carolina 27695-7905, USA

Cathodes based on $LiCoO_2$ that contain various lithium-conducting species (lithium hectorite, lithium Laponite, and lithium-exchanged Nafion) are studied in conjunction with lithium metal anodes and composite electrolytes based upon lithium hectorite clays as the charge carrier. Performance is compared to that of cells with a standard liquid electrolyte (*i.e.*, $LiPF_6$ +1:1 w/w ethylene carbonate:ethyl methyl carbonate). Effects on cathode capacity are examined for these variables: hot-press force used in construction of the porous cathode, carbon type (graphite *vs.* carbon black), and clay particle size. AC impedance spectroscopy is used to probe the cells and equivalent circuits are used to model the physical processes that occur. Cathodes containing 4 wt % lithium hectorite +3 wt % lithium-exchanged Nafion +3 wt % carbon black exhibit discharge capacities approximately 90 mAh/g $LiCoO_2$ compared to that observed in a standard cell of 110 mAh/g $LiCoO_2$. These clay-containing cathodes are potentially attractive for use in single-ion conducting lithium-ion batteries designed for high discharge applications.
 [DOI: 10.1149/1.1579034]

Manuscript submitted March 6, 2002; revised manuscript received January 15, 2003. Available electronically May 30, 2003.

Single-ion conducting electrolytes present a unique alternative to traditional lithium battery electrolytes. A lithium-ion transference number of unity would eliminate concentration-polarization losses in the cell, resulting in an increase in maximum power. Simulation has shown that a unity lithium-ion transference number may offset an order of magnitude drop in conductivity in high-discharge applications.[1] However, this predicted advantage of high lithium-ion transference number electrolytes has yet to be demonstrated experimentally, as few electrolytes with both high lithium-ion transference numbers and moderate room-temperature conductivities ($>10^{-4}$ S/cm) have been studied, let alone operated in lithium-metal or lithium-ion cells.

In a true single-ion conducting electrolyte where the anionic species is immobile, the conducting species will not penetrate presently formulated porous electrodes made for traditional liquid electrolytes; high electrode/electrolyte impedance and essentially no capacity would result due to the small area of electrode/electrolyte contact. Composite electrodes must be developed that incorporate a single-ion conducting species into the electrode structure to permit access of Li^+ to the active sites and maintain low impedance.

Deng *et al.*[2] reported lithium batteries using a polymeric single-ion conductor (a blend of poly(ethylene glycol) dimethyl ether, poly(sulfohexyl methacrylate lithium), and poly[methoxy oligo(oxyethylene) methacrylate-*co*-acrylamide], with a room-temperature conductivity approximately 3.5-5.5 $\times$ 10^{-6} S/cm) and a cathode consisting of vanadium oxide ($Li_{1-x}V_3O_8$) blended with the polymer single-ion conductor. The authors note good shelf stability of these cells, but the cell performance is limited by what they believe to be poor charge-transfer kinetics at the polymer single-ion conductor/vanadium oxide interface. More recent work reports polymer single-ion conducting electrolytes with higher conductivities ($>10^{-4}$ S/cm).[3-5] Though the authors expect to see lithium-ion transference numbers of unity, values were either not reported[3,4] or were observed to be low (<0.3) and explained by reaction of the solvent with the lithium metal electrodes which created other mobile ionic species.[5]

We previously reported composite electrolytes based on lithium hectorite in high dielectric organic solvents [ethylene carbonate (EC) and propylene carbonate (PC)] that possess room-temperature conductivities of approximately 2×10^{-4} S/cm.[6] Lithium-ion transference numbers of these clay-based electrolytes were observed greater than 0.95, as measured by the steady-state current method.[6] In addition, these composites show mechanical stability (elastic modulus, $G' > 10^5$ Pa and dynamic yield stress $>10^3$ Pa for 25 wt % Li hectorite composites) and shear-thinning behavior (desirable for processing).[7]

Demonstration of these electrolytes in full lithium-ion cells requires the development of composite anodes and cathodes which incorporate a single-ion conductor throughout the electrode structure. This single-ion conductor may or may not be of the same composition as the bulk electrolyte. The nature of the particles comprising the electrode may dictate to an extent the single-ion conductor that will achieve peak performance. For example, a hydrophilic electrode particle may be best served by using a hydrophilic single-ion conductor and vice versa. Likewise, the size and shape of the electrode particle may dictate what size and shape of single-ion particulate conductor should be used. The single-ion conductor should most likely be much smaller than the electrode particles to maximize the electrode/electrolyte interfacial contact area.

This paper examines composite electrodes based on lithium cobolt oxide ($LiCoO_2$) cathodes that incorporate single-ion conducting species into the porous structure. The electrodes are studied in ''pseudo'' lithium-ion half-cells with a lithium hectorite-based composite electrolyte and a lithium metal counter electrode.

Experimental

Synthetic sodium hectorite from Hoechst Celanese (SKS-21, 88 mequiv/100 g, 250 nm av size, average charge/particle approximately 65,000) was ion exchanged to the lithium form, rinsed, and dried, as described previously.[6] Dispersion in the carbonates [EC, PC, and dimethyl carbonate (DMC), Aldrich] and formation of the mixtures was carried out using deionized (DI) water as a dispersing aid. The resulting gel was dried to concentrated form and diluted as needed to the final desired concentration and composition. Water content of the clay-based electrolytes is approximately 150 ppm, as measured by Karl-Fischer titration.

Coin cells (Fig. 1) were assembled with $LiCoO_2$ cathodes (Alfa). Graphite (Timrex SFG 6 special graphite, Timcal America) or carbon black (Vulcan XC72R, Cabot) was added to the cathodes to promote electronic conductivity. Lithium foil (Aldrich) was employed as the anode. A poly(vinyl difluoride) (PVDF) binder (Kynar, Elf Atochem) and 1-methyl-2-pyrolidinone solvent (Aldrich) were employed in casting the electrodes onto aluminum foil using methods previously described.[8] Electrodes are approximately 1.3 cm diam and 100 μm thick. Individual cathodes were hot pressed at approximately 150°C in a heated platen hydraulic press at pressures ranging from 700 to 2800 bar. We refer to these cathodes as well as cells containing these cathodes as standard cathodes or standard cells, respectively.

* Electrochemical Society Student Member.
** Electrochemical Society Active Member.
z E-mail: fedkiw@eos.ncsu.edu

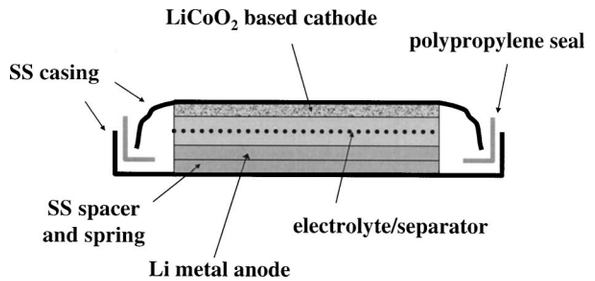

Figure 1. Schematic of coin cell.

Cathodes for use with the lithium hectorite-based electrolytes were produced by incorporating one or more of the following single-ion conducting species into the $LiCoO_2$ cathodes: Li hectorite, Li Nafion (lithium-exchanged Nafion) and Li Laponite (Laponite, Southern Clay Products, approximately 78 mequiv/100 g, 25 nm av size, average charge/particle approximately 850, lithium-exchanged by methods similar to those used for the hectorite[6]). Solvents used for blending and casting various composite cathodes are shown in Table I. Carbon black (or graphite) and PVDF weight percents were not optimized for any of the cathodes, but held constant from one cathode composition to the next. The composite cathodes were cast, pressed, and dried in the same manner as the standard cathodes. The water content of the cathodes was determined by Karl-Fisher titration to be less than 10 ppm.

The electrolyte employed for composite cathode cell-cycling studies was 0.5 M Li hectorite in PC (0.48 g Li hectorite/g PC with conductivity approximately 2×10^{-4} S/cm) dispersed in a polypropylene mesh separator (McMaster Carr, approximately 500 μm thick with 50% open volume). The standard electrolyte chosen for comparison is 1 M $LiPF_6$ in 1:1 w/w EC:ethyl methyl carbonate (EMC) (EM Industries; conductivity approximately 9×10^{-3} S/cm). Celgard 2400 polypropylene separator (Hoechst Celanese, approximately 20 μm thick) was used for liquid electrolytes.

Typically, two coin cells for each cathode composition were assembled in an argon-filled glove box for study by cell cycling and impedance spectroscopy. Cell cycling was performed on an Arbin BT2042 battery tester. Charge/discharge currents of 1 and 0.1 mA (0.8 and 0.08 mA/cm^2) were used on the standard and clay-based cells, respectively, unless otherwise noted. The lower current was typically used with the clay-based cells to compensate for the higher electrolyte resistance due to the lower electrolyte conductivity and thicker separator employed. Cutoff voltages were 4.2 V for charge and 2.5 V for discharge. Cell impedance was monitored periodically at the end of the fourth charge cycle (unless otherwise noted) using a BAS-Zahner IM6e impedance analyzer. Frequency range and amplitude for the impedance measurements were set at 1 MHz to 100 mHz and 10 mV, respectively. Impedance was generally measured at the end of the charge cycle rather than the discharge cycle so as to keep the impedance contribution due to lithium transport within the $LiCoO_2$ particles to a minimum and avoid possible masking of the impedance contributions of the lithium-ion transport through the electrode pores and the charge-transfer kinetics at the $LiCoO_2$ interface.

An equivalent circuit for the standard cell (Fig. 2a) was chosen based on the model proposed by Thomas *et al.* for a $LiCoO_2$ cathode and 1 M $LiBF_4$:PC electrolyte.[9] Their model consists of elements in series representing the bulk electrolyte resistance (R_e), a surface layer at the cathode (surface layer resistance, R_{sl}, and capacitance C_{sl}), and the cathode; the circuit for the cathode consists of a combination of a charge-transfer resistance (R_{ct}) in series with a Warburg impedance (W), representing a faradaic process, which are parallel with a series combination of a constant-phase element (CPE, Q) and double-layer capacitance (C_{dl}), representing nonfaradaic processes. We add a resistance and capacitance for the lithium-electrolyte film to their model (R_{Li} and C_{Li}, respectively). The equivalent circuit model for cells containing clay particulates is similar to that used for the standard cells but with two additional capacitive elements, the first representing the capacitance of the bulk clay-based electrolyte (C_e) and the second representing the capacitance of the clay-based electrolyte in the cathode (C_h) (Fig. 2b).

The ZsimpWin software (Princeton Applied Research) was used to fit the equivalent circuit elements to the impedance data. Nonlinear least-squares fitting was used to determine values for the model parameters. A common difficulty observed with the equivalent-circuit fitting was the existence of multiple minima. For a given set of impedance data, more than one combination of values for the proposed equivalent circuit would provide a visually acceptable fit. The converged parameter set was often dependent on the initial

Table I. Typical cathode compositions and procedures for blending the components prior to casting onto aluminum foil current collector.

Cathode composition	Solvent(s) used	Blending procedure
Standard 94 wt % $LiCoO_2$ 3 wt % carbon black 3 wt % PVDF	1-methyl-2-pyrolidinone (NMP)	PVDF is mixed in NMP then added to $LiCoO_2$/carbon black mixture
3-7 wt % Li Nafion 3 wt % carbon black 90-94 wt % $LiCoO_2$	alcohol/water mixture (AW)	Li Nafion is mixed in the AW then added to $LiCoO_2$/carbon black mixture
4 wt % Li hectorite (or 4 wt % Li Laponite or 2 wt % Li hectorite +2 wt % Li Laponite) 3 wt % carbon black 3 wt % PVDF 90 wt % $LiCoO_2$	*N*,*N*-dimethyl acetimide (DMAC) ethylene carbonate (EC)	Li hectorite (or Li Laponite or Li hectorite + Li Laponite) is dispersed in EC, added to PVDF/DMAC mixture, then mixed with $LiCoO_2$/carbon black mixture
4 wt % Li hectorite 3 wt % Li Nafion 3 wt % carbon black 90 wt % $LiCoO_2$	EC or water (AW)	Li hectorite is dispersed in either EC or water, mixed with Li Nafion/AW, then mixed with $LiCoO_2$/carbon black mixture

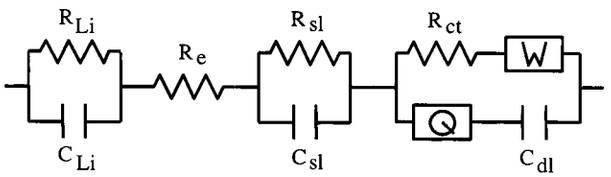

(a) Standard Cell Equivalent Circuit

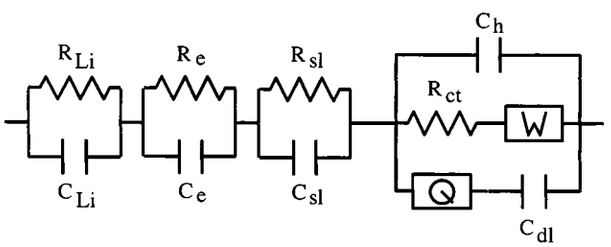

(b) Composite Cell Equivalent Circuit

Figure 2. Equivalent circuit model used for (a) standard and (b) clay-based cells. R_{Li}: lithium-electrolyte film resistance; C_{Li}: lithium-electrolyte film capacitance; R_e: electrolyte resistance; C_e: clay-based electrolyte capacitance; R_{sl}: cathode-electrolyte surface-layer resistance; C_{sl}: cathode-electrolyte surface-layer capacitance; R_{ct}: cathode charge-transfer resistance; W: Warburg impedance ($Z_W = A_W(j\omega)^{-1/2}$); Q: constant phase element ($Z_Q = A_Q(j\omega)^{-n}$); C_{dl}: double-layer capacitance; C_h: clay-based electrolyte capacitance in cathode.

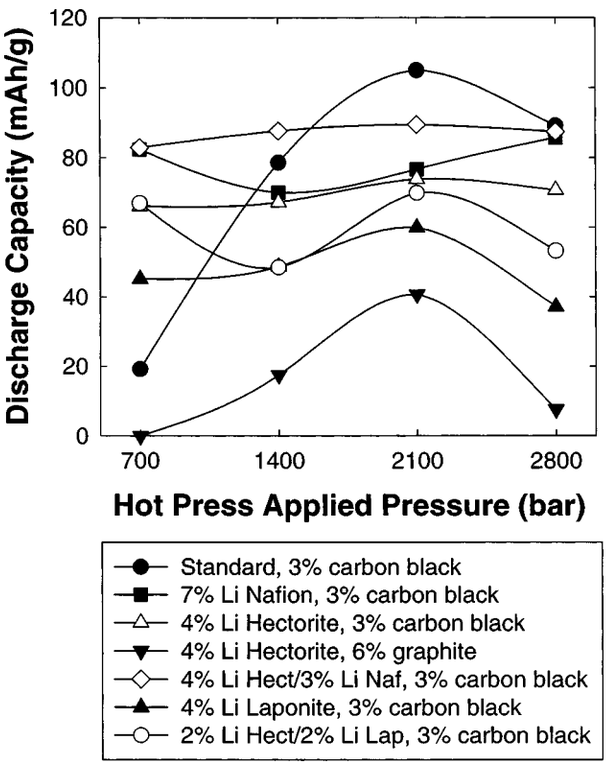

Figure 3. Effect of compaction pressure used in forming cathode on specific discharge capacity. Standard cells use a 1 M $LiPF_6$, 1:1 wt/wt EC:EMC electrolyte, while the clay-based cells use a 0.5 M Li hectorite, PC electrolyte (approximately 32 wt % Li hectorite). Cathodes were pressed at 150°C for approximately 5 s. Capacity reported is of the first discharge cycle.

values chosen to begin the iterative fit. As a means to circumvent these difficulties and provide a consistent approach, the general technique employed in this study was to first fit a simple circuit containing only resistive and capacitive elements to the impedance data, then use these parameters as initial values in an expanded model (containing the Warburg impedance and CPE). The numerical values of the parameters were also examined to insure their reasonableness. For instance, the approximate value of the electrolyte resistance could be estimated knowing the electrolyte conductivity and separator thickness and porosity. If the bulk electrolyte resistance obtained from the data fit was not reasonably close to the estimated value, the model was considered either invalid or converged to an incorrect minimum. Additionally, if parameter values were observed that were not realistic (for example, a capacitor of 5.75×10^{14} F was fit in one instance), the fit and/or model was not considered valid. As a cross check, parameter values from cell 1 of a specific cathode composition were used as initial values for cell 2 of the same cathode composition and vice versa. Parameters from this cross check convergence were observed to be virtually identical (within 1%) to those obtained from the original convergence.

Results

Single-ion conducting cathode capacity.—The effect of compaction pressure on the first-cycle specific discharge capacity of various cathodes is presented in Fig. 3. The standard-formulation electrodes contained 3 wt % carbon black and were cycled with a standard 1 M $LiPF_6$/1:1 wt/wt EC:EMC electrolyte at 0.8 mA/cm^2 (approximately C/2.5 rate). The effect of compaction pressure on capacity for the standard electrodes was significant, showing a maximum specific capacity near 110 mAh/g at 2100 bar.

Single-ion conducting cathodes containing various combinations of Li hectorite, Li Laponite, and Li Nafion were cycled with a 0.5 M Li hectorite/PC electrolyte (0.48 g Li hectorite/g PC) at 0.08 mA/cm^2 (approximately C/25 rate). The effect of compaction pressure on first-discharge capacity was less significant for single-ion conducting electrodes containing 3 wt % carbon black, and in some cases no specific effect of compaction pressure was observed. However, the cathode containing 4 wt % Li hectorite +6 wt % SFG 6 graphite showed a pronounced effect of compaction pressure, similar to that observed with the standard cathodes. Specific capacities were observed as high as 90 mAh/g for cathodes containing 4 wt % Li hectorite +3 wt % Li Nafion +3 wt % carbon black at pressures of 2100 bar.

The clay-containing cathodes were also evaluated at C/2.5 in cells with the standard 1 M $LiPF_6$/1:1 wt/wt EC:EMC electrolyte to verify that a fair performance comparison is made between the standard and clay-containing cathodes (Fig. 4). With the exception of the lowest compaction pressure studied (700 bar), the clay-containing electrodes generally exhibited performance equal to or less than that of the standard electrodes. Access to the $LiCoO_2$ surface for lithium transfer in the clay-containing electrodes is presumably then at best equivalent to that in the standard electrodes. The lower performance is expected, as any clay particles occluding the $LiCoO_2$ surface restrict access to the liquid electrolyte. At the lowest compaction pressure, the clay may be exhibiting binding properties and thereby attenuate the effect of interparticle conductivity losses at the low-compaction pressures. Ultimately, the addition of clay to the cathodes did not appear to have either significantly altered the cathode pore structure or improved electrolyte access to the $LiCoO_2$ surface.

Figure 5 further illustrates the effect of carbon type on specific discharge capacity. In standard cells, there was no significant effect of carbon type on cathode capacity at the carbon loadings studied; capacities of cathodes with graphite or carbon black were approximately 110 mAh/g. Likewise, there was no significant effect of carbon type on the capacities of Li Nafion-containing electrodes, with both capacities being approximately 75 mAh/g. However, in cathodes containing Li hectorite, there was a significantly higher capacity observed in cathodes containing carbon black at 3 wt % *vs.* graphite at 6 wt %. For example, the capacity in cathodes containing

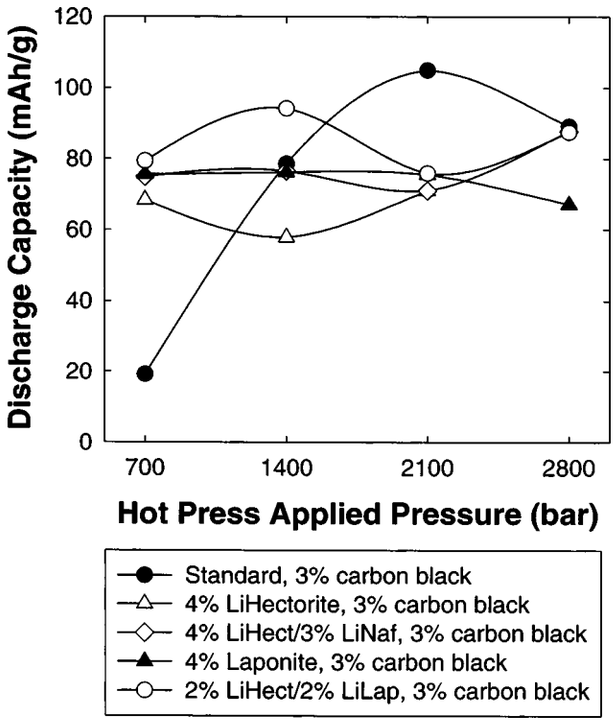

Figure 4. Effect of clay addition and binder substitution (Li Nafion for PVDF) on $LiCoO_2$-based cathode specific discharge capacities. All cathodes were evaluated using a 1 M $LiPF_6$, 1:1 wt/wt EC:EMC electrolyte. Cathodes were pressed at 150°C for approximately 5 s. Capacity reported is of the first discharge cycle.

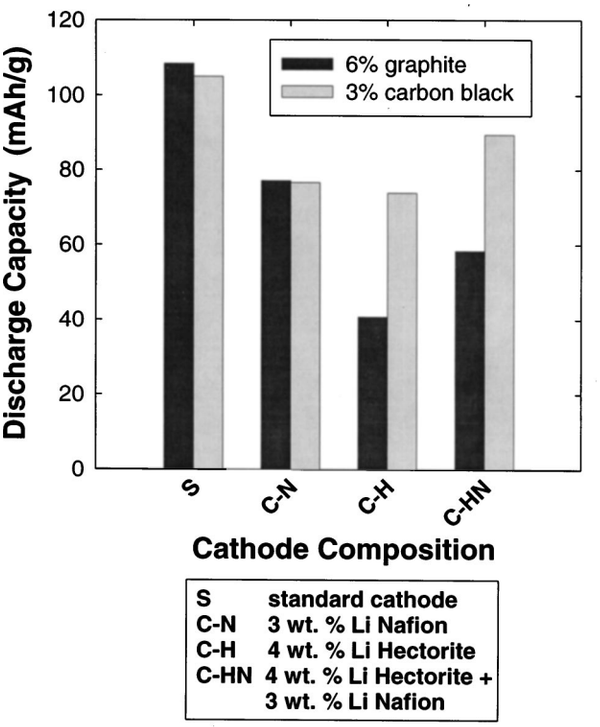

Figure 5. Effect of carbon type (SFG 6 graphite *vs.* carbon black) on cathode specific discharge capacity. Capacity reported after first discharge cycle. Standard cells use a 1 M $LiPF_6$, 1:1 wt/wt EC:EMC electrolyte, while the clay-based cells use a 0.5 M Li hectorite, PC electrolyte (approximately 32 wt % Li hectorite). Capacity reported is of the first discharge cycle.

4 wt % Li hectorite increased from approximately 40 mAh/g in the graphite-containing cathodes to nearly 75 mAh/g in the carbon black-containing cathodes. In cathodes containing 4 wt % Li hectorite +3 wt % Li Nafion, a similar increase was observed, from approximately 55 to 90 mAh/g.

To further improve lithium-ion transport at the electrolyte/cathode interface, a smaller clay was examined. Laponite (Southern Clay Products) is a synthetic hectorite approximately a factor of ten smaller than that obtained from Hoechst (25 *vs.* 250 μm) but with a lower cation-exchange capacity (approximately 78 *vs.* 88 meq/100 g). The effect of clay particle size on the clay-containing cathode specific capacity is presented in Fig. 6. The capacity of a 4 wt % Li Laponite cathode is approximately 60 mAh/g compared to a capacity of approximately 75 mAh/g for the 4 wt % Li hectorite cathode. Cathodes containing an equal mixture of the two (2 wt % Li hectorite +2 wt % Li Laponite) show a capacity just under 70 mAh/g, or nearly in the middle of the capacities of cathodes containing a single clay.

Cycling behavior and impedance.—Cycling behavior of two standard replicate cells for the first three cycles is shown in Fig. 7. Initial specific discharge capacities of both cells are above 100 mAh/g. Cell 1 shows significantly more fading than cell 2 with a specific discharge capacity of about 90 mAh/g at the third cycle while that of cell 2 remains above 100 mAh/g. Impedance measurements of both cells are similar (Fig. 8), with the minor differences most likely a result of typical variations in the cell composition and construction. Parameters for the circuit model used to fit the standard cell data are given in Table II, and the resulting fit is illustrated in Fig. 8. Bulk electrolyte resistance (R_e), resistance across the lithium passivation film (R_{Li}), and resistance at the $LiCoO_2$-electrolyte interface (R_{ct}) at open-circuit conditions for these cells are all on the order of 5 Ω cm^2. The limiting resistance of the standard cells appears to be the charge-transfer resistance at the $LiCoO_2$/electrolyte interface, of the order 200 Ω cm^2.

The results of cycling cathodes containing 4 wt % Li hectorite +6 wt % SFG 6 graphite are shown in Fig. 9. The two replicate cells show different initial capacities and fading behavior, with cell 1 exhibiting an initial specific discharge capacity close to 37 mAh/g and fading to 32 mAh/g on the third cycle, while cell 2 shows an initial discharge capacity greater than 50 mAh/g and little fading after three cycles. Impedance measurements of the two cells are presented in Fig. 10. Cell 1 impedance was measured in the charged state (after the fourth charge cycle) while cell 2 impedance was measured in the discharged state (after the third discharge cycle).

Bulk electrolyte resistance (R_e), lithium-electrolyte film resistance (R_{Li}), and cathode/electrolyte surface layer resistance (R_{sl}) were similar for the replicate 4 wt % Li hectorite +6 wt % SFG 6 graphite cells at full charge and discharge (Table II). Charge-transfer resistance (R_{ct}) for the discharged cell (cell 2) was significantly higher than that for the charged cell (cell 1). The Warburg prefactor, A_w, increased significantly from the charged cell 1 to the discharged cell 2, while the CPE prefactor, A_Q, is lower in cell 2 than cell 1. Upon comparing equivalent circuit parameter values for the 4 wt % Li hectorite +6 wt % SFG 6 graphite cell in the charged state (cell 1) with those of the standard cell, it is obvious that all resistive components for the clay-based cell were significantly higher than those for the standard cell. A discussion of these parameters is presented in the next section.

Cycling behavior and impedance measurements of two replicate cells with cathodes containing 4 wt % Li hectorite +3 wt % carbon black are shown in Fig. 11 and 12, respectively. Again, as with the graphite-containing cells, there is some variability between the two replicates. Cell 1 shows an initial specific discharge capacity less than 75 mAh/g, but discharge capacity fades to near 60 mAh/g with the third cycle. Cell 2 shows an initial capacity around 80 mAh/g

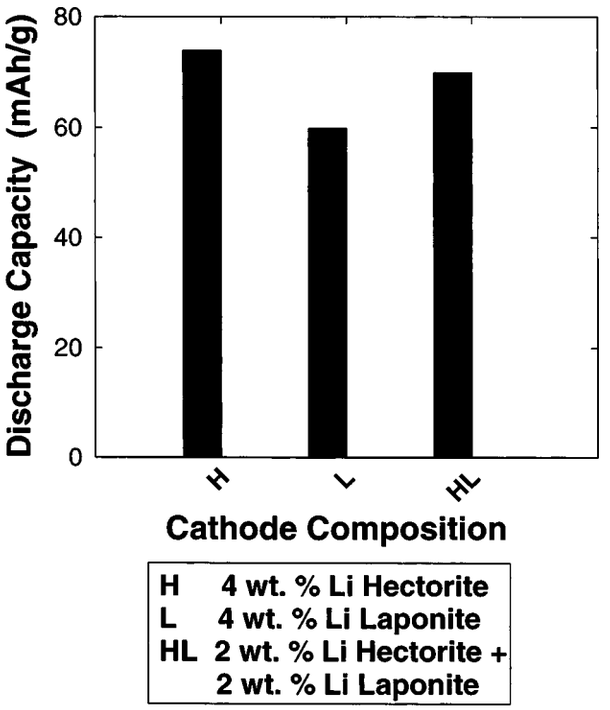

Figure 6. Effect of lithium-exchanged clay particle size on clay-containing cathode specific discharge capacity. Primary particle sizes of the hectorite and Laponite are approximately 250 and 25 nm, respectively. Capacity reported after first discharge cycle. A 0.5 M Li hectorite, PC electrolyte (approximately 32 wt % Li hectorite) is used.

and only fades to 75 mAh/g at the third cycle. Cell 2 exhibits both a lower R_{ct} (1080 *vs.* 1430 Ω cm^2) and a lower A_Q (606 *vs.* 758 Ω cm^2) compared to cell 1 (Table II). Once again, resistance values for the clay-based cells are considerably higher than those for the standard cells. However, the CPE prefactor (A_Q) is considerably lower

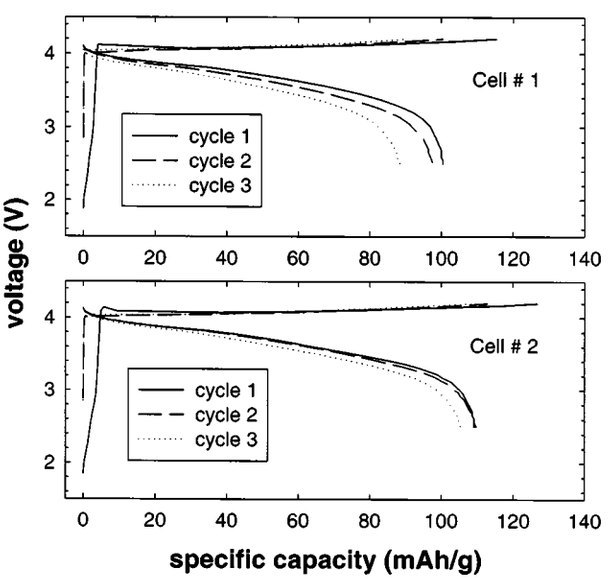

Figure 7. Cycling behavior of standard cells. Cathode composition is 94 wt % $LiCoO_2$ +3 wt % carbon black +3 wt % PVDF. Electrolyte is 1 M $LiPF_6$ in 1:1 wt/wt EC:EMC solvent. Charge/discharge rate is 0.8 mA/cm^2 (approximately C/2.5 rate).

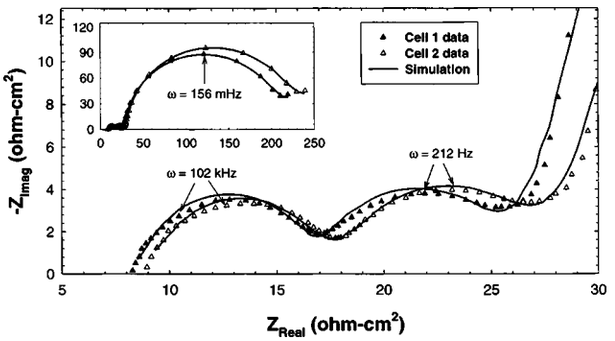

Figure 8. Standard cell impedance at full charge. Cathode composition is 94 wt % $LiCoO_2$ +3 wt % carbon black +3 wt % PVDF. Electrolyte is 1 M $LiPF_6$ in 1:1 wt/wt EC:EMC solvent. Impedance is measured after fourth charge cycle.

(approximately 2.5-4 times) for the 4 wt % Li hectorite +3 wt % carbon black cathodes compared to the 4 wt % Li hectorite +6 wt % graphite cathodes.

Cathodes containing 4 wt % Li hectorite +3 wt % Li Nafion +3 wt % carbon black exhibit the highest capacities of all the single-ion conducting cathodes examined. Cycling behavior of two replicate cells containing these cathodes is shown in Fig. 13. These cells are more alike than any of the other single-ion conducting electrode replicates presented. Cell 1 shows an initial specific discharge capacity greater than 90 mAh/g and fades to 85 mAh/g with the third cycle, and cell 2 shows an initial capacity of 90 mAh/g and also fades to 85 mAh/g with the third cycle. Impedance measurements of the two cells after the fourth charge cycle are similar (Fig. 14), as well as the equivalent circuit parameters (Table II). Cell 2 seems to exhibit a slightly lower cathode R_{ct} but a slightly higher value for the CPE prefactor (A_Q). Addition of Li Nafion to the cathode seems to improve cell capacity by lowering both the cathode R_{ct} and R_{sl} compared to the other clay-containing cathodes examined. Once again, however, resistances are higher for the Nafion-containing cathodes relative to the standard cathodes.

Impedance for a single-ion conducting cell in which the cathode contains only Li Nafion as the single-ion conductor (7 wt % Li Nafion +3 wt % carbon black) is shown in Fig. 15. Corresponding data for the equivalent-circuit parameters is reported in Table II. The cathode surface-layer resistance (R_{sl}) for this cell is higher than that with cathodes containing 4 wt % Li hectorite +3 wt % Li Nafion. Additionally, A_Q is lower than that with cathodes containing 4 wt % Li hectorite +3 wt % Li Nafion, and the Warburg prefactor, A_w, is lowest among all the single-ion conducting cells.

Discussion

The data show that the processing history and/or composition of cathodes affect its capacity significantly. For example, consider the effect of compaction pressure on a standard cathode (Fig. 3). At low compaction pressure (<2100 bar), interparticle contact is not good and electronic conductivity is poor, resulting in low capacity. At high compaction pressure (>2100 bar), the pores of the cathode collapse and electrolyte cannot adequately penetrate the structure, resulting in a low interfacial-contact area between the electrolyte and cathode, again reducing capacity. A maximum in capacity is therefore observed when compaction pressure is large enough to produce good interparticle contact without collapsing the pore structure. For the compositions observed in this study, the optimum compaction pressure is near 2100 bar.

With single-ion conducting cathodes containing hectorite, the effect of compaction pressure depends on the cathode composition. The effect of high-compaction pressure (>2100 bar) on the capacity of these cathodes can be dramatic, as with the 4 wt % Li hectorite +6 wt % graphite cathode in which the capacity drops to 5

Table II. Equivalent circuit parameters for standard and clay-based cell models. Best fit for cell impedance measured at end of fourth charge cycle, unless otherwise noted.

	Standard		4% Li hectorite +6% graphite		4% Li hectorite +3% carbon black		4% Li hectorite +3% Li Nafion +3% carbon black		7% Li Nafion +3% carbon black
	Cell 1	Cell 2	Cell 1	Cell 2[a]	Cell 1	Cell 2	Cell 1	Cell 2	Cell 1
R_e (Ω cm^2)	6.15	4.62	387	291	293	279	281	320	301
C_e (nF/cm^2)			0.922	0.851	1.15	0.969	0.801	0.790	0.911
R_{Li} (Ω cm^2)	6.19	5.42	71.5	63.3	42.8	20.4	49.3	41.9	27.6
C_{Li} (μF/cm^2)	0.594	0.349	2.07	1.46	19.0	3.25	2.58	5.42	10.9
R_{sl} (Ω cm^2)	5.50	5.16	164	135	73.4	107	48.5	55.5	200
C_{sl} (μF/cm^2)	108	126	376	4.08	1740	1140	0.0151	0.0160	5750
R_{ct} (Ω cm^2)	182	202	1140	3680	1430	1080	884	737	536
A_W (Ω cm^2/s$^{1/2}$)	8.93	9.80	21.7	143	45.5	34.5	22.7	25.0	8.70
A_Q (Ω cm^2/s^n)	15.8	21.4	2620	1700	758	606	461	550	840
$n(0 < n < 1)$	0.120	0.095	0.225	0.255	0.103	0.086	0.188	0.182	0.197
C_{dl} (mF/cm^2)	4.84	4.64	0.0994	0.335	1.21	1.07	1.08	0.954	0.209
C_h (nF/cm^2)			2.46	8.31	1.87	2.80	203	220	3.23

[a] End of third discharge cycle.

mAh/g at 2800 bar (Fig. 3). At lower compaction pressure (<2100 bar), it is more difficult to achieve good electronic conduction through these cathodes, resulting in capacities near zero at 700 bar. At high compaction pressures, in addition to pore collapse, we believe the plate-shaped hectorite particles are forced, on average, parallel to the platens and, hence, into an orientation perpendicular to the desired transport of the lithium cations. This impedes lithium-ion transport through the cathode. In addition, this orientation may also inhibit solvent transport into the cathode during cell assembly.

Changing the carbon type in these single-ion conducting cathodes from graphite to carbon black increases cathode capacity significantly (Fig. 5) and reduces the influence of compaction pressure on capacity. These effects are believed to be due to the size and shape of carbon black as compared to graphite. The SFG 6 graphite is lamellar-shaped with an average size of 6 μm. In contrast, the XC72R carbon black is composed of aggregated clusters (of the order 250 nm) of small primary particles with average size of 30 nm.[10] We believe that the branched structure of carbon black, as well as a particle size similar to hectorite, helps prevent alignment of the plate-like hectorite perpendicular to the applied compaction force (which would hinder lithium-ion transport), and promotes a more random orientation of the hectorite particles in the cathode structure. The randomly oriented clay particles in these carbon black/clay composites may also help prevent or limit cathode pore collapse at higher applied pressures by providing structural enhancement.

Carbon black in the single-ion conducting cathodes seems to improve the capacity at low-compaction pressure (<2100 bar) compared to single-ion conducting cathodes with graphite, such as the graphite/Li hectorite-containing cathode. This improvement in capacity at low-compaction pressure is not observed with the standard cathodes. However, clay-containing cathodes evaluated with the standard $LiPF_6$ electrolyte exhibit improved capacity at low compaction pressure compared to nonclay-containing cathodes. This combination of results suggests that the clay has binding properties, thereby attenuating the effect of compaction pressure, particularly at low compaction pressures where electronic conductivity loss due to poor interparticle contact lowers cathode capacity. The carbon black enhances this binding property by preventing clay platelet aggregation and maintaining a high-surface area for binding.

Even though the charge density of the Laponite is slightly lower than that of hectorite, we anticipated that the smaller Laponite clay

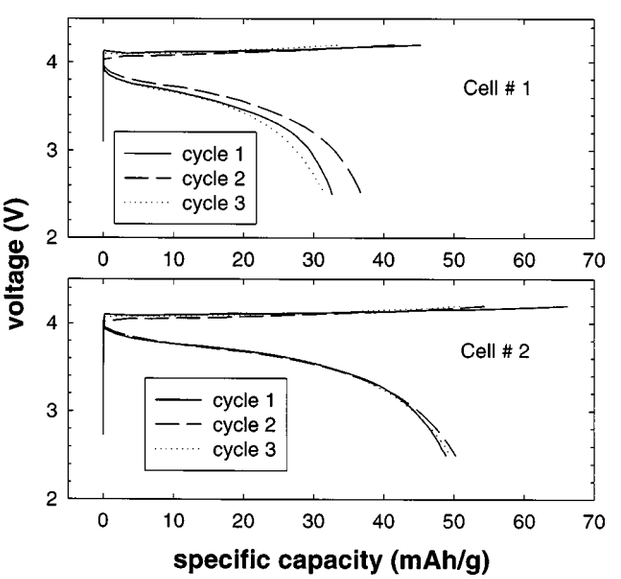

Figure 9. Cycling behavior of clay-based cells. Cathode composition is 87 wt % $LiCoO_2$ +4 wt % Li hectorite +6 wt % SFG 6 graphite +3 wt % PVDF. Electrolyte is 0.5 M Li hectorite in PC solvent. Charge/discharge rate is 0.08 mA/cm^2 (approximately C/25 rate).

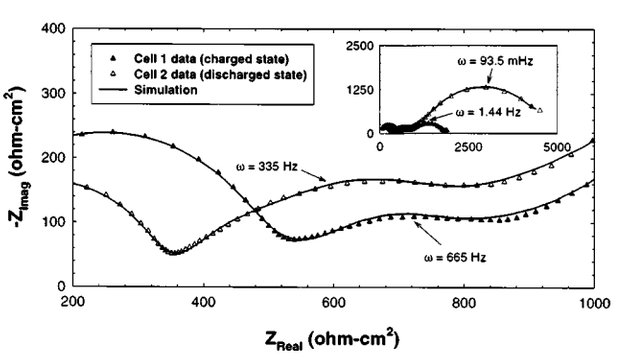

Figure 10. Clay-containing cathode cell impedance. Cathode composition is 87 wt % $LiCoO_2$ +4 wt % Li hectorite +6 wt % SFG 6 graphite +3 wt % PVDF. Electrolyte is 0.5 M Li hectorite in PC solvent. Impedance of cell 1 is measured after fourth charge cycle. Impedance of cell 2 is measured after third discharge cycle.

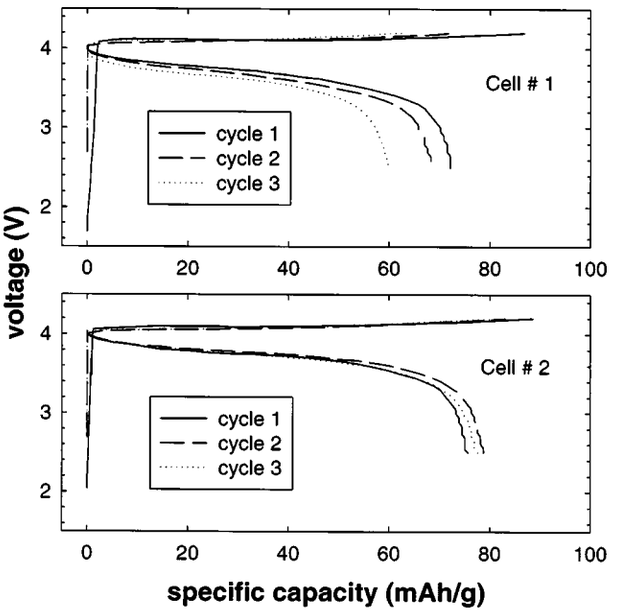

Figure 11. Cycling behavior of clay-based cells. Cathode composition is 87 wt % $LiCoO_2$ +4 wt % Li hectorite +3 wt % carbon black +3 wt % PVDF. Electrolyte is 0.5 M Li hectorite in PC solvent. Charge/discharge rate is 0.08 mA/cm^2 (approximately C/25 rate).

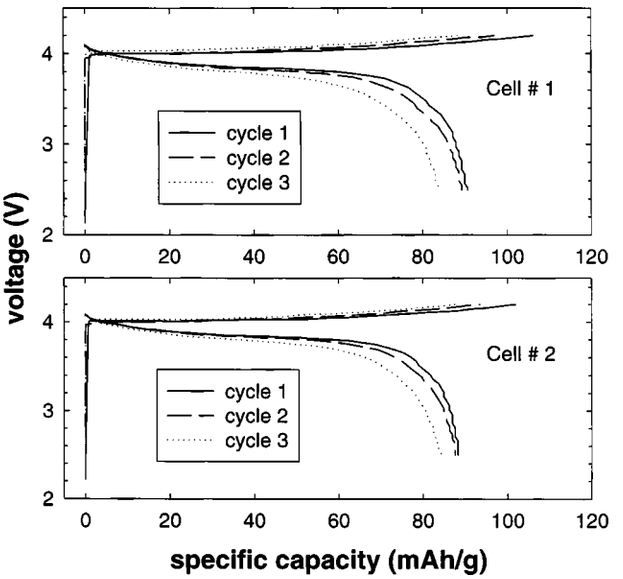

Figure 13. Cycling behavior of clay-based cells. Cathode composition is 87 wt % $LiCoO_2$ +4 wt % Li hectorite +3 wt % Li Nafion +3 wt % carbon black. Electrolyte is 0.5 M Li hectorite in PC solvent. Charge/discharge rate is 0.08 mA/cm^2 (approximately C/25 rate).

particle would improve the clay-containing cathode capacity *vs.* the hectorite-only counterparts. However, the results indicate otherwise (Fig. 6). We hypothesize that it is more difficult to disperse and maintain dispersion of the smaller Laponite particles, even at the relatively low concentrations used in the clay-containing cathodes. Thus, lithium-ion transport through the electrolyte and at the electrode/electrolyte interface is reduced.

The cell impedance and parameters from an equivalent-circuit fit of the data yields further insight into the differences between the standard and clay-containing cathodes, as well as between different compositions of the clay-containing cathodes. Comparing the clay-based cells to the standard cells, it is obvious that all equivalent-circuit resistances are higher for the clay-based cells *vs.* the standard cells. The R_e is expected to be higher for the clay-based cells given the lower electrolyte conductivity (2×10^{-4} *vs.* 9×10^{-3} S/cm) and thicker separator (500 *vs.* 20 μm) of the clay-based cells compared to the standard cells. The R_{Li} is also higher for the clay-based cells compared to the standard cells. This was not expected as lithium-lithium coin cells previously produced in our work for lithium-ion transference number measurements with clay-containing and standard electrolytes exhibited similar lithium/electrolyte interfacial impedances.[6] The lithium/electrolyte interfacial resistance observed in the clay-based cells is similar to that observed in clay-based transference number cells, while the lithium/electrolyte interface in the standard cells is lower than that observed in the standard transference number cells. The current densities used in the transference number measurements were at least an order of magnitude lower than used in this study and were applied for much shorter times (less than an hour compared to approximately three days). Dendrite formation at the lithium/electrolyte interface could be more significant in the standard cells, increasing the lithium/electrolyte surface area and in turn lowering the interfacial resistance. Conversely, the gelled clay-based electrolyte may inhibit dendrite formation.[11]

The higher values of R_{sl} and R_{ct} in the clay-based cells *vs.* the standard cells (Table II) indicate a more difficult transport of lithium ions across the bulk electrolyte/porous electrode interface and at the cobalt oxide particle interface in a single-ion conducting system.

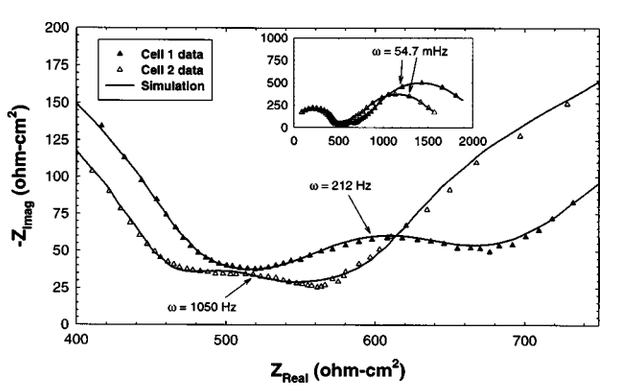

Figure 12. Clay-containing cathode cell impedance at full charge. Cathode composition is 87 wt % $LiCoO_2$ +4 wt % Li hectorite +3 wt % carbon black +3 wt % PVDF. Electrolyte is 0.5 M Li hectorite in PC solvent. Impedance is measured after fourth charge cycle.

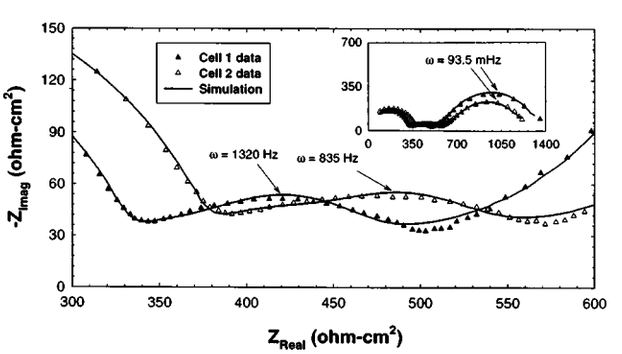

Figure 14. Clay-containing cathode cell impedance at full charge. Cathode composition is 87 wt % $LiCoO_2$ +4 wt % Li hectorite +3 wt % Li Nafion +3 wt % carbon black. Electrolyte is 0.5 M Li hectorite in PC solvent. Impedance is measured after fourth charge cycle.

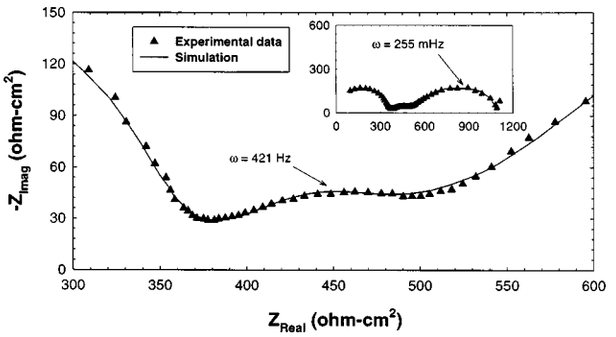

Figure 15. Nafion-containing cathode cell impedance at full charge. Cathode composition is 87 wt % $LiCoO_2$ +7 wt % Li Nafion +3 wt % carbon black. Electrolyte is 0.5 M Li hectorite in PC solvent. Impedance is measured after fourth charge cycle.

This observation is not surprising as the lithium ions in a standard liquid electrolyte have greater freedom of motion than in a single-ion conducting electrolyte due to the mobility of the anionic species. A more readily accessible surface area for lithium-ion transport at both interfaces is more easily achieved with a standard liquid electrolyte than with a single-ion conducting electrolyte.

The CPE Q is intended to capture the nonfaradaic ionic current in the electrode pores as well as the in-solid electronic current, *i.e.*, through the $LiCoO_2$ and carbon particles.[9] The value of the exponent, n, tending toward zero rather than one indicates that this element is dominated by a resistance rather than a capacitance; at $n = 0$, Q describes a resistor, while at $n = 1$, Q describes a capacitor.[12] Thus, the value of the CPE prefactor A_Q provides an indication of electronic and/or ionic resistance throughout the electrode, although it is not possible with this analysis to distinguish between the two. The significant increase in A_Q for the clay-based cell *vs.* the standard cells indicates significantly lower electronic and/or ionic conduction in the clay-containing cathode. The conductivity of the clay-based electrolyte is an order of magnitude lower than the standard electrolyte (approximately 2×10^{-4} *vs.* 9×10^{-3} S/cm), suggesting reduced ionic conduction in the clay-containing electrode pores. The clay in the cathode may also be disrupting the electronic pathways, possibly by blocking contact between any of the electronic current-carrying species (graphite or carbon black and cobalt oxide).

The impedances for the 4 wt % Li hectorite +6 wt % graphite cell were measured and modeled in the charged (cell 1) and discharged (cell 2) states. As expected, some parameters remained essentially unchanged, namely, R_e and R_{sl}. Other parameter values changed with the state of charge, as expected. In the discharged state in which lithium ions are intercalated into the cobalt oxide structure, it becomes difficult to insert more lithium ions, leading to higher R_{ct}.

Thomas *et al.* attribute the Warburg impedance to diffusion of the insertion ion in both the electrolyte and the electrode (in the intercalation region).[9] With a single-ion conducting electrolyte, diffusion resistance in the electrolyte would be nonexistent, and the Warburg impedance would simply be representative of the insertion ion in the intercalation cathode. In the discharged state, the interlayer structure is saturated with lithium cations, resulting in higher resistance to diffusion (*vs.* the charged state of the cell) and hence a higher A_w and Warburg impedance.

The value of A_Q is 35% lower for cell 2 (discharged) *vs.* cell 1 (charged). Thus, the cathode in cell 2 appears to have better electronic and/or ionic pathways than the cathode in cell 1. The electronic resistance of $Li_{1-x}CoO_2$ varies with state of charge. However, at full discharge ($x = 0$) the electronic resistance is at its highest,[13] counter to the change in A_Q observed for the two cells. Thus, the difference in A_Q between cell 2 and cell 1 appears to be rooted in the ionic pathways of the two cathodes. The hectorite particulates in the cathode of cell 2 may be better distributed than in cell 1, a result likely attributed to variations in the production of the cathodes. This helps explain the improved capacity observed in cell 2 *vs.* cell 1 (Fig. 9).

Cycling behavior of the clay-based cells depends strongly on the electrode composition. One would expect a capacity increase with more efficient dispersion of the single-ion conducting species throughout the electrode. Improved dispersion of the single-ion conductor should be reflected in a decrease in interfacial impedance (or R_{sl}) because the lithium-ion transport across the electrode/electrolyte interface is improved. Likewise, R_{ct} should decrease with improved dispersion of the single-ion conductor. Both of these effects are observed in the parameters from the equivalent-circuit models of the various clay-containing cathodes. The 4 wt % Li hectorite +3 wt % Li Nafion+3 wt % carbon black cathode cells exhibit the highest capacities and also the lowest values for R_{sl} and R_{ct} among the clay-containing cathodes studied. Likewise, these cells exhibit the most consistent initial-discharge capacities across a wide cathode compaction-pressure range (700-2800 bar). The addition of Li Nafion as a binding agent to the cathode, with both hydrophilic and hydrophobic features, rather than hydrophobic PVDF, may help promote hectorite dispersion in addition to providing additional lithium-ion charge carriers.

The 4 wt % Li hectorite +3 wt % Li Nafion +3 wt % carbon black cathodes, in addition, exhibit the lowest values for A_Q, indicating the least resistive electronic and/or ionic pathways in the cathode among the clay-containing cathodes studied. This is another indication of improved hectorite dispersion in the cathodes. Cathodes containing carbon black (*i.e.*, 4 wt % Li hectorite +3 wt % Li Nafion +3 wt % carbon black and 4 wt % Li hectorite +3 wt % carbon black) exhibit A_Q values that are approximately 2.5-5 times lower than cathodes containing graphite (*i.e.*, 4 wt. % Li hectorite +6 wt % graphite). The role that the carbon black may play in promoting hectorite dispersion and preventing hectorite alignment has been mentioned, both of which should enhance ionic conduction in the cathode pores. The branched structure and smaller dimensions of the carbon black may also help reduce loss in electronic conductivity with addition of hectorite to the cathode. In addition to alignment of hectorite platelets under pressure, the platelets may preferentially align along the $LiCoO_2$ particle surfaces, as both are hydrophilic, and subsequently reduce the electronic contact area of the $LiCoO_2$ particles. The smaller size of the carbon black compared to the graphite may make the carbon black less susceptible to this surface-blockage effect.

In one instance, Li Nafion was fully substituted for Li hectorite in the single-ion conducting cathode. The two single-ion conductors have similar cation-exchange capacities: 0.91 mequiv/g for Nafion and 0.88 mequiv/g for hectorite. Upon comparing the equivalent-circuit parameters for the 7 wt % Li Nafion +3 wt % carbon black cathodes to those for the 4 wt % Li hectorite +3 wt % Li Nafion +3 wt % carbon black cathodes (Table II), Li Nafion improves charge transfer at the $LiCoO_2$ interface (lower R_{ct} for the all Nafion-containing cathode), although at the expense of both the electrode/bulk electrolyte surface-layer resistance (higher R_{sl} for the all Nafion-containing cathode) and ionic/electronic transport in the cathode (higher A_Q for the all Nafion-containing cathode). We hypothesize that the Li Nafion orients preferentially with the hydrophilic sulfonic branches toward the hydrophilic $LiCoO_2$ (improving charge transfer, but lowering ion transport through the cathode) and the hydrophobic backbone toward the carbon black (possibly blocking the carbon black from creating an optimum electronic pathway). Additionally, the dissimilarity of the lithium-ion conducting phases of the all Nafion-containing cathode and hectorite-based bulk electrolyte (compared with a cathode containing hectorite) results in more difficult lithium-ion transport across the interface and thus a higher R_{sl} than any of the hectorite-containing cathodes.

Differences in cathode performance for replicates of the same cathode composition correlate with equivalent-circuit modeling. For example, of the two cells containing the 4 wt % Li hectorite +3 % carbon black, cell 1 exhibits a lower capacity and a higher capacity fade than cell 2 (Fig. 11). Not surprisingly, cell 2 exhibits a lower R_{ct} and lower A_Q compared to cell 1.

Conclusions

Cathodes for use with single-ion conducting electrolytes have been demonstrated with a clay-based electrolyte consisting of 0.5 M lithium hectorite in PC (approximately 32 wt % Li hectorite). Initial optimization of some variables (carbon type and hot-press force) yielded cathodes comprised of 4 wt % Li hectorite +3 wt % Li Nafion +3 wt % carbon black +90 wt % $LiCoO_2$ with a first-discharge capacity of approximately 90 mAh/g compared to a standard cathode capacity of approximately 110 mAh/g.

Carbon black in the clay-containing cathode is preferred to graphite; it is believed that the branched structure and small (approximately 30 nm) primary particle size of the carbon black prevents the Li hectorite platelets from aligning perpendicular to the direction of lithium-ion transport during the hot-press formation of the cathode. This, in turn, should improve ionic conduction in the clay-containing cathodes with carbon black compared to those with graphite. Lower values of A_Q for the clay-containing cathodes with carbon black *vs.* graphite obtained from the equivalent-circuit model agree with this hypothesis.

Addition of Li Nafion to the clay-containing cathodes improved both the dispersion of the clay, resulting in improved ionic transport, and reduced charge-transfer resistance. However, complete substitution of Nafion for the clay seemed to reduce ionic transport in the cathode electrolyte and to increase the resistance at the hectorite-based bulk electrolyte/cathode interface. The Nafion provided a better charge transfer at the $LiCoO_2$ surface most likely due to the flexible nature of the polymer providing the ability to conform to the particle surface. On the other hand, the Nafion may be aligned with the hydrophilic sulfonic groups near the hydrophilic $LiCoO_2$ surface, resulting in poor lithium-ion transport in the electrode pores and at the bulk-electrolyte/cathode interface. The rigid structure of the clay did not allow for good conformation at the $LiCoO_2$ surface, but allowed for better lithium-ion transport throughout the bulk of the pores and at the electrode/electrolyte interface. Thus, the hectorite and the Nafion both played integral roles in the transport processes in the single-ion conducting cathodes. The bulk electrolyte resistance of the clay-based cells was considerably higher than that of the standard liquid electrolyte cells, but this is expected given the thickness of the separator employed in the clay-based cells compared to the standard cells (500 *vs.* 20 μm). The focus of our work is on the single-ion conducting cathode behavior so bulk electrolyte resistance was not a concern; nevertheless, electrolyte resistance can be reduced by utilizing thinner, more porous separator materials with the clay-based electrolyte. However, other resistances in the clay-based cells, namely, cathode charge-transfer resistance, cathode electronic/ionic resistance, and electrolyte/cathode surface-layer resistance were also considerably higher than those in the standard cells and must be reduced if full-cell performance at higher currents is to be realized. Single-ion conductors must be incorporated into typical lithium-ion anodes (graphites) as well.

Acknowledgments

This work was supported, in part, by the NCSU Hoechst-Kenan program and the Air Force Office of Scientific Research through the U.S. Department of Defense National Defense Science and Engineering Fellowship Program. In addition, the authors thank Barrie Davies for his insight and intellectual support in this work.

North Carolina State University assisted in meeting the publication costs of this article.

References

1. M. Doyle, T. Fuller, and J. Newman, *Electrochim. Acta*, **39**, 2073 (1994).
2. Z. Deng, Q. Xu, Y. Zheng, and G. Wan, *J. Power Sources*, **50**, 369 (1994).
3. M. Guglielmi, P. Aldebert, and M. Pineri, *J. Appl. Electrochem.*, **19**, 167 (1989).
4. M. Watanabe, Y. Suzuki, and A. Nishimoto, *Electrochim. Acta*, **45**, 1187 (2000).
5. Z. Florjanczyk, W. Bzducha, J. R. Dygas, B. Misztal-Faraj, and F. Krok, *Solid State Ionics*, **119**, 251 (1999).
6. M. W. Riley, P. S. Fedkiw, and S. A. Khan, *J. Electrochem. Soc.*, **149**, A667 (2002).
7. M. W. Riley, P. S. Fedkiw, and S. A. Khan, *Mater. Res. Soc. Symp. Proc.*, **575**, 137 (1999).
8. J. Fan and P. S. Fedkiw, *J. Power Sources*, **72**, 165 (1998).
9. M. G. S. R. Thomas, P. G. Bruce, and J. B. Goodenough, *J. Electrochem. Soc.*, **132**, 1521 (1985).
10. Cabot Corporation North American Technical Report S-136.
11. J. Zhou, P. S. Fedkiw, and S. A. Khan, *J. Electrochem. Soc.*, **149**, A1121 (2002).
12. *Impedance Spectroscopy. Emphasizing Solid Materials and Systems*, J. R. Macdonald, Editor, p. 91, John Wiley & Sons, New York (1987).
13. N. Imanishi, M. Fujyoshi, Y. Takeda, O. Yamamoto, and M. Tabuchi, *Solid State Ionics*, **118**, 121 (1999).